



FOCUS: MALDI-TOF AND BIOLOGICAL MS: RESEARCH ARTICLE

# MALDI Mass Spectrometric Imaging of Lipids in Rat Brain Injury Models

Joseph A. Hankin,<sup>1</sup> Santiago E. Farias,<sup>1</sup> Robert M. Barkley,<sup>1</sup> Kim Heidenreich,<sup>1</sup> Lauren C. Frey,<sup>3</sup> Kei Hamazaki,<sup>2</sup> Hee-Yong Kim,<sup>2</sup> Robert C. Murphy<sup>1</sup>

<sup>1</sup>Department of Pharmacology, University of Colorado Denver, Aurora, CO, USA

<sup>2</sup>Laboratory of Molecular Signaling, NIAAA, National Institutes of Health, Bethesda, MD, USA

<sup>3</sup>Department of Neurology, University of Colorado Denver, Aurora, CO, USA

## Abstract

Matrix-assisted laser desorption ionization/ionization imaging mass spectrometry (MALDI IMS) with a time-of-flight analyzer was used to characterize the distribution of lipid molecular species in the brain of rats in two injury models. Ischemia/reperfusion injury of the rat brain after bilateral occlusion of the carotid artery altered appearance of the phospholipids present in the hippocampal region, specifically the CA1 region. These brain regions also had a large increase in the ion abundance at  $m/z$  548.5 and collisional activation supported identification of this ion as arising from ceramide (d18:1/18:0), a lipid known to be associated with cellular apoptosis. Traumatic brain injury model in the rat was examined by MALDI IMS and the area of damage also showed an increase in ceramide (d18:1/18:0) and a remarkable loss of signal for the potassium adduct of the most abundant phosphocholine molecular species 16:0/18:1 (PC) with a corresponding increase in the sodium adduct ion. This change in PC alkali attachment ion was suggested to be a result of edema and influx of extracellular fluid likely through a loss of Na/K-ATPase caused by the injury. These studies reveal the value of MALDI IMS to examine tissues for changes in lipid biochemistry and will provide data needed to eventually understand the biochemical mechanisms relevant to tissue injury.

**Key words:** MALDI, IMS, Imaging mass spectrometry, Sublimation, Brain, Phosphatidylcholine, Ceramide, Traumatic brain injury, Ischemia reperfusion, Brain injury, Alkali metal adduct images, CA1, Hippocampus damage

**Abbreviations:** CID collision-induced dissociation; DHB 2,5-dihydroxybenzoic acid; MALDI IMS matrix-assisted laser desorption/ionization imaging mass spectrometry; PC phosphatidylcholine; TOF time of flight; FPI fluid percussion injury; Cer ceramide (long chain base:N-acyl chain)

## Introduction

The coupling of advanced time-of-flight mass spectrometers with MALDI has facilitated the development of

imaging mass spectrometry (MALDI IMS) for mapping specific molecules present in animal and plant tissues. Analyte ions are produced directly from a tissue slice coated with MALDI matrix and sequential masses are acquired across the entire tissue surface. The use of the time of flight (TOF) analyzer permits the rapid acquisition of all ions generated from a nanosecond laser photon pulse over a broad mass range with high mass resolution. Thus, a unique data set can be obtained where spatial distribution at 10–100  $\mu\text{m}$  lateral resolution of the tissue for a set of very diverse molecules is

**Electronic supplementary material** The online version of this article (doi:10.1007/s13361-011-0122-z) contains supplementary material, which is available to authorized users.

Correspondence to: Robert C. Murphy; e-mail: Robert.Murphy@ucdenver.edu

Received: 28 January 2011  
Revised: 1 March 2011  
Accepted: 2 March 2011  
Published online: 9 April 2011

revealed. Much of the extensive development over the past decade has been in the area of peptide and protein detection from the laboratory of Caprioli [1], but more recently this approach has been extended to studies of the distribution of complex lipids and drugs in biological tissues in many applications including cancer research [2], neuroscience [3, 4], and drug discovery and development [5].

Perhaps not unexpectedly, the most abundant ions observed below  $m/z$  1500 in the MALDI IMS experiment of tissues such as brain [6], kidney [7], liver [8], eye [9], and blood vessels [10] were derived from those lipids that make up the various membranes of the living cell (phospholipids and sphingolipids) as well as lipid storage vesicles found in abundance in certain cell types. The most abundant positive ions typically observed are derived from a single class of lipid called phosphatidylcholine (PC), but within that class are numerous molecular species that differ from each other by fatty acyl group esterification to the glycerophosphocholine backbone. Much of the image diversity revealed in MALDI IMS relates to the distribution of individual phospholipid molecular species in specific tissue regions. Detailed studies have now revealed that there is a good correlation between the abundance of MALDI IMS-derived ions and the local concentration of individual PC molecular species but, on the other hand, there is bias against other phospholipid classes such as phosphatidylethanolamine, phosphatidylinositol, and phosphatidylserine molecular species as positive ions [11]. These latter lipid classes yield abundant negative ions while PC does not.

The use of imaging of lipids by mass spectrometry to reveal biological phenomena is in its very beginnings, but the work of Burnum et al. [12] has revealed that this technology can be invaluable in understanding complex lipid changes in vivo. The work described here builds on the number of studies of lipid distribution in the brain of rodents, which are rich in lipids and regional lipid diversity. Brain injury models in conjunction with MALDI IMS were previously used to study perturbation in such diverse lipid profiles [3, 13]. We show here that MALDI IMS can reveal unique localized biological events related to lipid biochemistry that are initiated by CNS injury.

## Materials and Methods

The 2,5-dihydroxybenzoic acid (DHB) was purchased from Sigma Aldrich Chemical Company (St. Louis, MO, USA) and all organic solvents were purchased from Fisher Scientific (Fair Lawn, NJ, USA). Phospholipid and ceramide standards were purchased from Avanti Polar Lipids (Alabaster, AL, USA).

### *Traumatic Brain Injury Model*

A fluid percussion injury (FPI) model in rats was employed as previously described [14, 15]. FPI involves a rapid injection of fluid through a small craniotomy made over the left parietal cortex. Subsequent to the injury, the animals were allowed to recover for 72–96 h before they were

anesthetized with isoflurane and decapitated. The brains were rapidly dissected out, mounted in the microtome cutting stage, and submerged in ice-cold HBSS buffer. The brains were then cut into 1–2 mm coronal slices at the visible site of injury. These slices were laid flat into a 1 in. square plastic pathology sample tray, flash-frozen in crushed dry ice, and subsequently stored at  $-80^{\circ}\text{C}$  until sectioning. Sections were cut coronally ( $10\ \mu\text{m}$ ) at  $-15^{\circ}\text{C}$  using a cryostat, mounted onto stainless steel MALDI insert plates (Applied Biosystems), and stored at  $-20^{\circ}\text{C}$  until MALDI IMS analysis. Adjacent sections were collected onto glass slides and stained with hematoxylin and eosin (H and E) for cellular morphology comparisons. Staining of several 1 mm sections with 2,3,5-triphenyltetrazolium chloride (TTC) was carried out independent of tissue collected for MALDI IMS to measure lesion volume following FPI [15, 16]. All animal experiments were approved by the Institutional Animal Care and Use Committee at the University of Colorado Denver.

### *Ischemic/Reperfusion Injury Model*

Sprague-Dawley rats (269–343 g, male) were purchased from Charles River Laboratories (Wilmington, MA, USA). As a stroke model, transient ischemia was induced by the bilateral occlusion of rat common carotid arteries. Animals were anaesthetized using halothane, and the tail artery was cannulated for blood pressure monitoring on the day of surgery. Rats were placed on a heated pad to maintain the body temperature at  $37^{\circ}\text{C}$ . Both common carotid arteries were isolated after a ventral midline neck incision and occluded for 20 min with nontraumatic micro-arterial clips. Simultaneously, the blood pressure was reduced to and maintained between 50 and 55 mmHg for the duration of the surgery by means of fine adjustments of the halothane anesthesia [17]. Four days after surgery, rats were euthanized, brains were collected, and  $10\ \mu\text{m}$  sections at 4.20 mm caudal to bregma were prepared for histology and lipid analysis. Brains from sham-operated animals were used as controls. This approach produced greater than 70% hippocampal cell death in the CA1 region with significant interneuronal atrophy when evaluated by toluidine blue staining. All experimental procedures were approved by the Animal Care and Use Committee of the National Institute on Alcohol Abuse and Alcoholism, National Institute of Health (LMS-HK02).

### *Matrix Application*

The MALDI plates containing the brain slices were coated with matrix (DHB) using sublimation [18]. The MALDI plate was attached to the condenser using double-sided thermally conductive tape (3M, St. Paul, MN, USA). Sublimation of DHB matrix took place in the sublimation chamber (0.05 Torr) with a condenser temperature of  $15^{\circ}\text{C}$ . DHB (275 mg) was added and heat was applied (42 V, heating mantle) for 11 min, which resulted in the deposition

of a thin, even layer of DHB matrix on top of the tissue sample.

### MALDI IMS

MALDI-TOF analysis used for tissue imaging was carried out on a QStar XL Qq-TOF instrument using Analyst QS software with o-MALDI Ser 5.1 (Applied Biosystems). A solid state high repetition laser (355 nm wavelength) operated at 500 Hz, 8.2  $\mu$ J, with a 0.243 s acquisition time was used for the traumatic brain injury imaging experiments and a nitrogen laser (335 nm wavelength, 20 Hz, 40  $\mu$ J, 0.5 s acquisition) was used for the ischemia/reperfusion study. The estimated pressure was 10 mTorr at the location of the MALDI plate during acquisition and 10-shots/pixel was used with the nitrogen laser and 120-laser shots/pixel with solid state laser. Conditions for acquisition in positive ion mode included a focusing potential (FP) of 60, declustering potential (DP2) 20, curtain gas of 25 units. Collisional activation experiments were carried out using argon as collision gas at 20 V. The ischemia/reperfusion injury studies involved separate analysis of the injured and non-injured hemispheres where images were acquired at 50  $\mu$ m plate movements using oversampling [19]. Each hemisphere took 12 h to acquire across the 12  $\times$  16 mm<sup>2</sup> area of tissue. The FPI experiment images were acquired at 75  $\mu$ m plate movement, and typically took 10–12 h to acquire across the 16  $\times$  14 mm<sup>2</sup> area of the sample surface. The MALDI data were processed from raw data to ‘analyze’ format using a ‘wiff to analyze’ script provided by Applied Biosystems/MDS SCIEX at a resolution of 10 data points/u and viewed using Tissue View software (Applied Biosystems).

Comparison of ion abundances were made between injured and non-injured regions by delineating a ‘region of interest’ within the mass spectrometric image of traumatic brain injury and control regions in each of four MALDI-MS images of tissue slices from four different experimental animals. The averaged signal intensity was extracted for each of the ions considered in this study, ratios calculated (signal from specific ions in the FPI region divided by the signal from these same ions from the contralateral control area), and averaged for four different experiments (Table 1). Standard error of the mean was calculated for  $n=4$  independent trials.

**Table 1.** Average ratio of the ion abundance, integrated in the region of injury, from molecular ion alkali metal adduct and protonated species (TBI injury side/contralateral side) for two abundant phosphatidylcholines ( $n=4$ )

Phospholipid species	Molecular ion species	Average ratio $\pm$ std error of the mean( $n=4$ )
16:0/16:0 PC [M+H] <sup>+</sup>	$m/z$ 734.5	0.93 $\pm$ 0.05
16:0/16:0 PC [M+Na] <sup>+</sup>	$m/z$ 756.5	1.33 $\pm$ 0.20
16:0/16:0 PC [M+K] <sup>+</sup>	$m/z$ 772.5	0.73 $\pm$ 0.05
16:0/18:1 PC [M+H] <sup>+</sup>	$m/z$ 760.5	0.95 $\pm$ 0.09
16:0/18:1 PC [M+Na] <sup>+</sup>	$m/z$ 782.5	1.28 $\pm$ 0.10
16:0/18:1 PC [M+K] <sup>+</sup>	$m/z$ 798.5	0.80 $\pm$ 0.06

## Results

### Positive Ion MALDI Images—Ischemia/Reperfusion Injury Model

Both sham-operated and experimentally infarcted rat brain sections were analyzed separately by MALDI IMS. As expected, the majority of positive ions observed in the MALDI IMS experiment were derived from lipids as evidenced by the significant mass defect (typically 0.5 to 0.8 u) for all major MALDI ions in the range  $m/z$  500–1000. Excellent images defining major regions of the brain were obtained as previously reported [18]. One of the brain regions most vulnerable to cerebral ischemia is the hippocampus, particularly the CA1 region, in both rodent models [20, 21] and humans [22, 23]. Therefore, it was not surprising that there was a loss of substructure definition in the hippocampus of the ischemic hemisphere along with an increase in discontinuous pits and holes in the tissue. This could be seen in the images of most PC molecular species as illustrated for the abundant ion at  $m/z$  760.6, palmitoyl-oleoyl-phosphatidylcholine (POPC) (Figure 1). When a comparison of the ion abundances of all MALDI ions from  $m/z$  400 to 1000 were made from just the hippocampal regions of control and ischemic brain sections (Figure 2a and b), the distribution of phospholipid molecular species,  $m/z$  700 to 850, previously identified in rat brain tissues were clearly similar. However a large increase in an ion at  $m/z$  548.5 was apparent in the spectrum of the ischemic hemisphere (Figure 2b), which now was the most abundant ion in this mass range of the injured brain. When the image of this ion in both control and injured hemispheres was generated (Figure 3), a distinct increase of the ion intensity was apparent in the CA1 region of the hippocampus (Figure 3b) of the injured brain. This ion was consistent with a unique ceramide (Cer d18:1/18:0), which appeared as a dehydrated product ion  $[M+H - H_2O]^+$  that likely formed under our tissue imaging conditions ([24], see below). Other molecular species of ceramides, including Cer (d18:1/16:0) at  $m/z$  520.5 and Cer (d18:1/16:1)  $m/z$  518.5, were observed located in this same region of the ischemic brain section, although in lower abundance. Alternatively, this ion could have been derived from a cerebroside, which is known to lose the sugar moiety to form a dehydrated ceramide ion. However, identification as a ceramide (see experiments below) was consistent with previous studies of lipids extracted from the gerbil hippocampus that had undergone similar brain ischemia and reported an increase in Cer (d18:1/18:0) by approximately 150% [25]. This is the first report of the highly localized formation of this bioactive lipid mediator in the CA1 region.

### Positive Ion MALDI Images—Traumatic Brain Injury (FPI Model)

Histologic staining of the brain slice taken at the site of FPI clearly revealed the site of damage using TTC, which stained viable cells pink but injured (dead or dying cells)

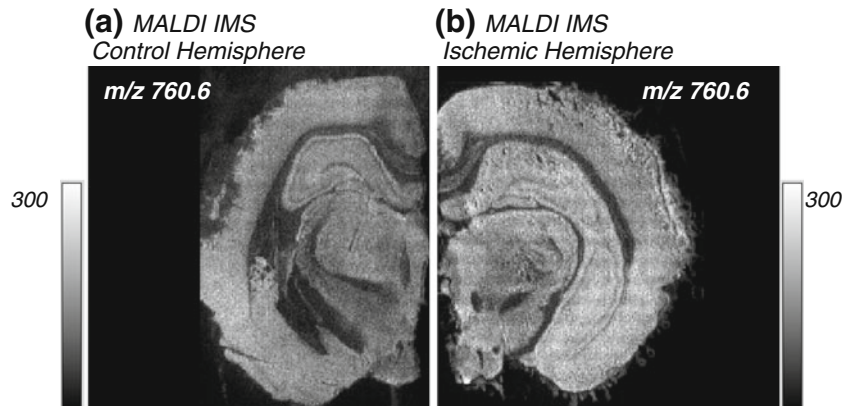


**Figure 1.** MALDI IMS representing palmitoyl-oleoyl phosphatidylcholine  $[M+H]^+$   $m/z$  760.6 in rat brain from **(a)** a single hemisphere from control animal; **(b)** a single hemisphere from animal subjected to bilateral ischemia

as white on the left side of the brain slice. There were no signs of trauma on the control hemisphere revealed by this staining protocol and using light microscopy (Figure 4a). The MALDI IMS experiment performed on the immediately adjacent slice revealed phospholipid distributions in the entire brain slice (data not shown) similar to those previously reported [26]. The most abundant PC molecular species present in the positive ion spectra were 16:0/16:0 PC ( $[M+H]^+$   $m/z$  734.5,  $[M+Na]^+$   $m/z$  756.5,  $[M+K]^+$   $m/z$  772.5), and 16:0/18:1 PC ( $[M+H]^+$   $m/z$  760.6,  $[M+Na]^+$   $m/z$  782.6,  $[M+K]^+$   $m/z$  798.6). The identity of these species have been confirmed by collisional activation studies [27], and although there are certainly other

isobaric ions present in the mix at each  $m/z$  value considered in this study, the species named have been found to be predominant. The MALDI IMS image of the most abundant PC molecular species ( $m/z$  760.6, 16:0/18:1-PC $[M+H]^+$ , Figure 4b) was surprising in that the abundance of this very common and very stable PC was apparently less in the region of injury. While this might indicate that the 16:0/18:1-PC was lost from this injury region, even a dead cell would be expected to retain an intact phospholipid bilayer and the associated PCs at the original site of the cell. Even if disruption of the cell membrane took place, it was unlikely that the PC would disappear so strikingly from this region of the brain.

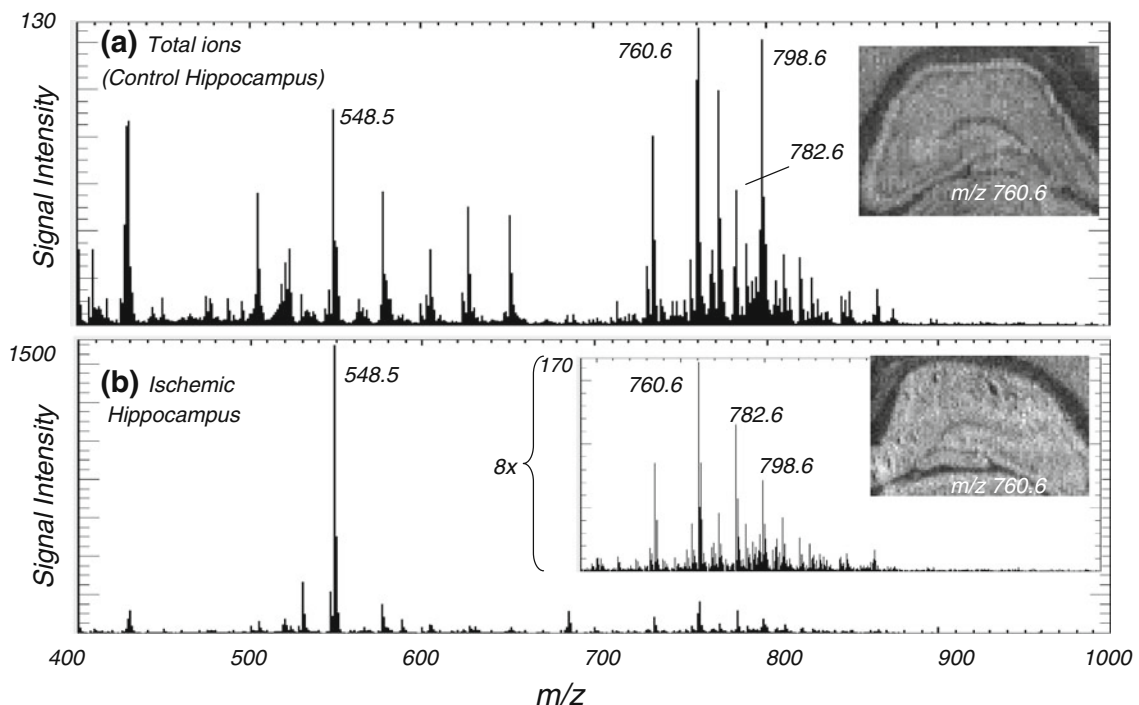


**Figure 2.** MALDI-TOF mass spectra averaged over the hippocampus region of the MALDI image of rat brain from **(a)** a single hemisphere of control animal; **(b)** a single hemisphere of animal subjected to bilateral ischemia. Inset: 8 $\times$  expansion of signal intensity scale for mass range  $m/z$  700–1000

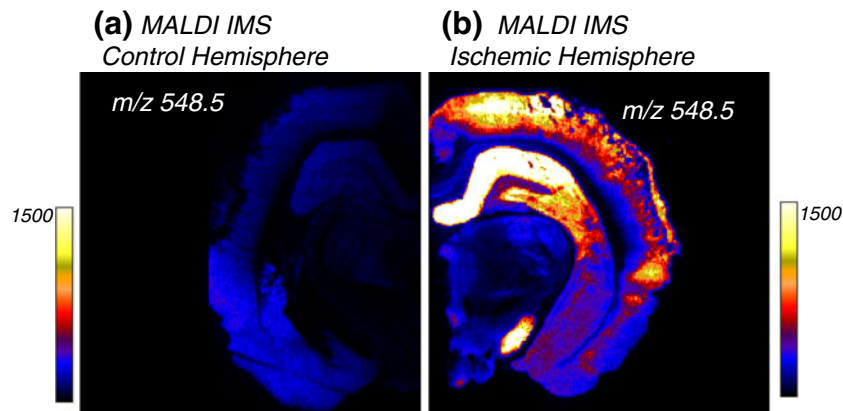


**Figure 3.** MALDI IMS representing  $m/z$  548.5 ( $[M+H - H_2O]^+$ , Cer [d18:0/18:1]) in rat brain from **(a)** single hemisphere of control animal; **(b)** single hemisphere of animal subjected to bilateral ischemia

Therefore, this PC molecular species was further examined by making images of the  $Na^+$  and  $K^+$  adduct ions which also were major ions in the MALDI IMS experiment.

The distribution for the sodium adduct of 16:0/18:1 PC  $[M+Na]^+$   $m/z$  782.6 (Figure 4c) displayed an increased intensity at the region of injury while the potassium adduct 16:0/18:1 PC  $[M+K]^+$   $m/z$  798.6 (Figure 4d) was depleted from the injury region. The pattern of alkali metal adducts for 16:0/16:0 PC,  $[M+Na]^+$  at  $m/z$  756.5 and  $[M+K]^+$  at  $m/z$  772.5 showed the same trend with increased sodium adduct and decreased potassium adduct ions (Table 1).

MALDI-MS images from another animal with a more severe FPI (70 PSI) and 96 h post-injury displayed the same pattern of increased sodium, decreased potassium adducts related to the traumatic brain injury, but deeper into the brain tissue (data not shown). The locus of damage would be expected to differ with injury severity, and variability in placement of the percussive device onto the rat skull, and depth of 10 micron section within a 3D locus of damaged tissue. The data from four different FPI experimental animals were combined to further characterize the observation of disparate alkali metal adduct distributions. A region of interest (ROI) was manually

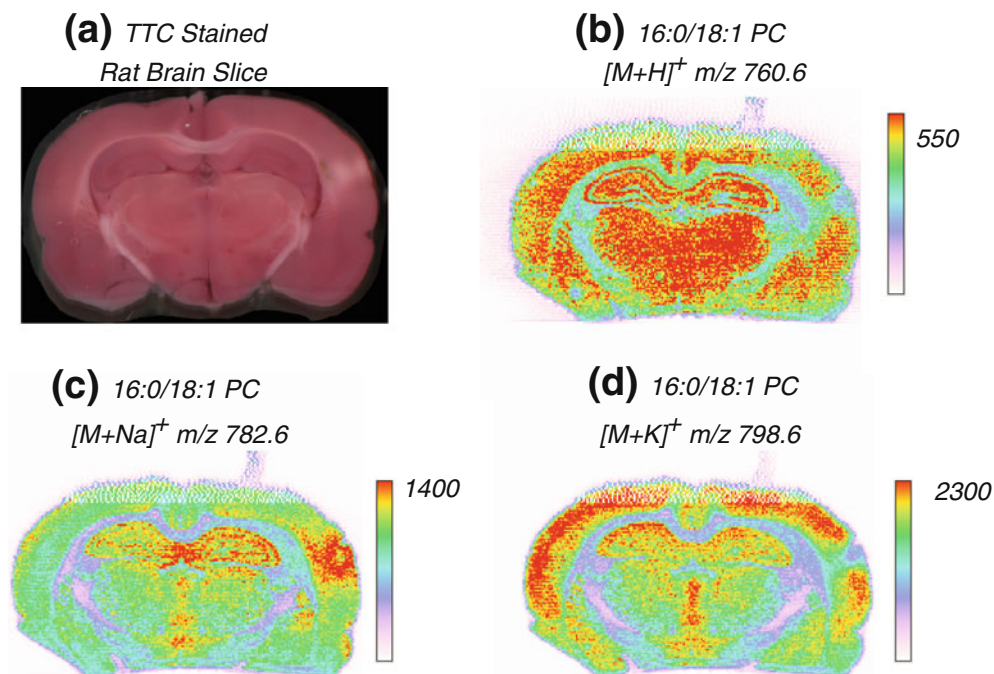


**Figure 4.** Rat brain sections from traumatic brain injury (TBI) model. **(a)** Tissue section stained with 2,3,5-triphenyl tetrazolium chloride (TTC); **(b)** MALDI IMS representing 16:0/18:1 PC  $[M+H]^+$   $m/z$  760.6; **(c)** MALDI IMS representing 16:0/18:1 PC  $[M+Na]^+$   $m/z$  782.6; **(d)** MALDI IMS representing 16:0/18:1 PC  $[M+K]^+$   $m/z$  798.6

drawn within the middle of the FPI damaged region observed in the MALDI-MS image, and a corresponding ROI of equal area was drawn within the control region. The averaged ratios of signal intensity (ions in the FPI region divided by ion signal of same ion in the contralateral control area) were calculated (Table 1). A consistent increase (20%–30%) in the intensity signal for the sodium adduct of both 16:0/16:0 PC and 16:0/18:1 PC is noted relative to the signal of the  $[M+H]^+$  species along with a corresponding decrease in the intensity signal for the potassium adduct.

Investigation of the traumatic brain injury image for the appearance of ceramide ions akin to observations made in the ischemia model (*vide supra*) revealed a focused distribution of an ion at  $m/z$  548.5 localized in the cortex and hippocampus of the injured hemisphere (Figure 5a). Collisional activation of this ion (Figure 5b) gave evidence of identity as a ceramide molecule with a characteristic product ion at  $m/z$  264.3 representing loss of the acyl chain, and rearrangement of the ceramide backbone [24, 28]. In separate experiments, vesicles prepared from an isotopically labeled ceramide standard, with POPC and cholesterol, were subjected to MALDI MS after application of DHB by sublimation. The Cer (d18:1/16:0 [ $^{13}C_4$ ])  $[M+H]^+$  at  $m/z$  542.5 was not observed but  $[M+Na]^+$  at  $m/z$  564.5 and  $[M+H - H_2O]^+$  at  $m/z$  524.5 were clearly present. Collisional activation of  $m/z$  524.5 in the vesicles yielded the characteristic  $m/z$  264 (Supplementary Figure 1). Another ceramide standard (Cer (d18:1/18:0-D<sub>3</sub>)  $[M+H]^+$   $m/z$  569.5 applied neat onto a MALDI plate and analyzed post DHB application by sublimation yielded no molecular ion, but  $[M+H - H_2O]^+$  at  $m/z$  551.5 as the prominent form. Collision-induced dissociation (CID) of the dehydrated ion at  $m/z$  551 yielded  $m/z$  264.3 as well. It is plausible the ion we observed at  $m/z$  548.5 ion MALDI images of damaged

brain tissue represents  $[M+H - H_2O]^+$  from Cer (d18:1/18:0).

## Discussion

The TOF mass analyzer is a powerful tool for collection of ions from the MALDI IMS experiment because all ions within a specific mass range can be collected after the laser initiation of the desorption process. These ions and their associated abundances can be assembled into a four-dimensional data base that can be examined off-line by many different tools, including construction of images revealing spatial distribution (x-y coordinates) specific for each mass-to-charge-ratio (molecule). Therefore, it is not surprising that advancement in TOF technology [29] has had an enormous impact on MALDI IMS. A second feature of MALDI IMS of animal tissues is that cellular lipids and in particular phospholipids are typically the most abundant ion species observed in the lower mass region of the MALDI IMS mass spectrum. This feature makes possible a new approach to examine lipid biochemistry that is not available to the lipid biochemist. While individuals studying proteins have extraordinarily powerful tools to visualize the location of a target protein using immunofluorescence and confocal microscopy or labeling a protein with a tag like green fluorescent protein, such approaches are not viable for studying small lipid molecules. Virtually all naturally occurring lipids lack fluorescent properties, but lipids do have unique properties of mass and accumulation in high numbers in membranes that define the compartments of cells. So, MALDI IMS can capitalize on these properties by using high resolution mass analyzers and focused laser desorption to yield IMS of these abundant lipid derived ion species.

Even though the formation of ceramides during ischemia reperfusion has been known for some time, the highly localized nature of their biochemical formation was not

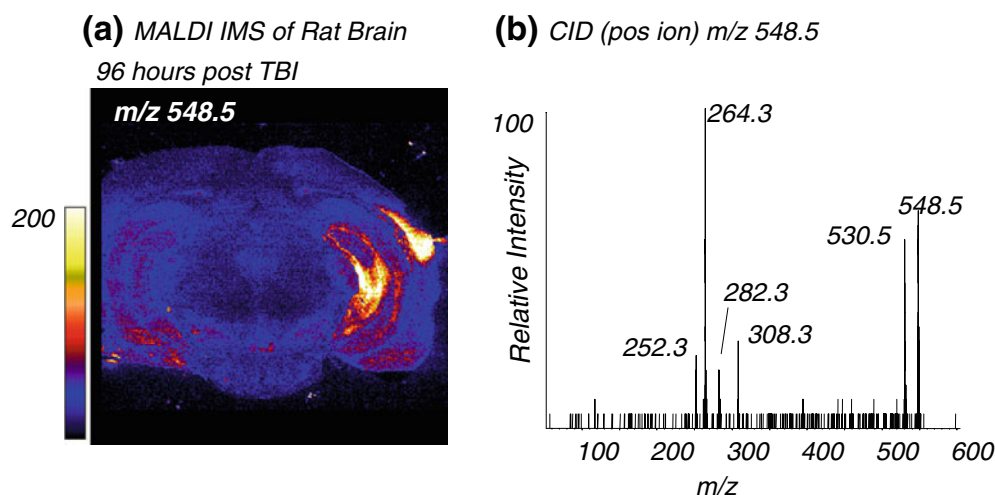


**Figure 5.** (a) MALDI IMS representing Cer (d18:0/18:1)  $[M+H - H_2O]^+$   $m/z$  548.5 in rat brain with unilateral TBI; (b) CID mass spectrum from  $m/z$  548.5 (on tissue)

previously reported. Ceramides are markers of dead or dying cells through cellular apoptosis and likely arise from the degradation of sphingomyelin after activation of a sphingomyelinase or from increase in *de novo* biosynthesis. It has been reported that ischemia/reperfusion decreased sphingomyelin levels and increased ceramide levels in gerbil hippocampus [25] and rat cortex [30]. Our MALDI IMS data showed a dramatic increase of the ceramide signal specifically in the CA1 region after ischemia, whereas no significant changes were seen in CA3. This is consistent with the fact that the CA1 region of the hippocampus is most susceptible to cerebral ischemia in both rodents and humans, while hippocampal CA3 region is remarkably resistant. Co-localized ceramide production and neuronal cell death in the CA1 region suggest that the sphingomyelin metabolism to ceramides may have a role in ischemic neuronal cell death in the hippocampus.

The MALDI IMS images using the fluid percussion model of traumatic brain injury revealed the altered distribution of alkali attachment ions ( $\text{Na}^+$  and  $\text{K}^+$ ) for the major PC molecular species at the region of injury. Since the rest of the brain served as control tissue for this experiment, this alteration in images for these two ions from the same phosphatidylcholine was a sensitive indicator of events taking place at the molecular level in the tissue environment. We suggest that the increase in  $\text{Na}^+$  that could occur during edema [31] and after loss of the  $\text{Na}^+/\text{K}^+$ -ATPase activity [32] and cell death would lead to the observed change in the MALDI IMS alkali attachment ion abundances. Our dry sublimation method preserved the alkali metal ions transferred to the tissues during the biochemical event, since the matrix added much later was deposited from the gaseous state [18]. Thus, the observed variability in net alkali metal attachment was most likely a measure of relative alkali metal concentration differences between two regions. What was even more surprising was that the extent of this disturbance in alkali metal concentration could be observed in the MALDI IMS images to be quite deep in the brain regions, well below the initial site of injury. This suggests that injury-induced biochemical events take place in the deeper brain regions, which may have significant implication in the overall traumatic brain injury outcome. Such subtle changes would be difficult to observe by other techniques but are readily observable when the image is taken as a whole.

In conclusion, the MALDI IMS of lipids in tissues and, specifically, in the brain yields enormous information about the occurrence of specific lipids. Details of biochemical events were visualized in the brain by this unique imaging technique as a result of injury. Ceramides were found to be produced in the hippocampal CA1 region after both ischemia/reperfusion injury and traumatic brain injury. Alteration in the concentrations of  $\text{Na}^+$  and  $\text{K}^+$  induced by traumatic brain injury could be visualized by the alkali metal adduct ions for these phospholipids. MALDI IMS enabling spatial visualization of the lipid profile in brain tissues

provides a powerful tool to study region-specific lipid biochemistry associated with brain injury.

## Acknowledgement

The authors acknowledge that this work was supported, in part, by a grant from the LipidMAPS Large Scale Collaborative grant from General Medical Sciences Institute (GM069338) of the National Institutes of Health and Colorado TBI Trust Fund. A part of this research (Kei H. and H.Y.K.) was supported by the intramural program of NIAAA, NIH. The authors thank Erin Genova (UC Denver Pathology Department) for assistance in preparation of FPI tissue sections.

## References

- Cornett, D.S., Rezyer, M.L., Chaurand, P., Caprioli, R.M.: MALDI Imaging Mass Spectrometry: Molecular Snapshots of Biochemical Systems. *Nat. Methods* **4**, 828–833 (2007)
- Schwamborn, K., Caprioli, R.M.: Molecular Imaging by Mass Spectrometry—Looking Beyond Classical Histology. *Nat. Rev. Cancer* **10**, 639–646 (2010)
- Koizumi, S., Yamamoto, S., Hayasaka, T., Konishi, Y., Yamaguchi-Okada, M., Goto-Inoue, N., Sugiura, Y., Setou, M., Namba, H.: Imaging Mass Spectrometry Revealed the Production of Lyso-Phosphatidylcholine in the Injured Ischemic Rat Brain. *Neuroscience* **168**, 219–225 (2010)
- Wisztorski, M., Croix, D., Macagno, E., Fournier, I., Salzet, M.: Molecular MALDI Imaging: An Emerging Technology for Neuroscience Studies. *Dev Neurobiol.* **68**, 845–858 (2008)
- Drexler, D.M., Garrett, T.J., Cantone, J.L., Deters, R.W., Mitroka, J.G., Prieto Conaway, M.C., Adams, S.P., Yost, R.A., Sanders, M.: Utility of Imaging Mass Spectrometry (IMS) by Matrix-Assisted Laser Desorption Ionization (MALDI) on an Ion Trap Mass Spectrometer in the Analysis of Drugs and Metabolites in Biological Tissues. *J. Pharmacol. Toxicol. Methods* **55**, 279–288 (2007)
- Sugiura, Y., Konishi, Y., Zaima, N., Kajihara, S., Nakanishi, H., Taguchi, R., Setou, M.: Visualization of the Cell-Selective Distribution of PUFA-Containing Phosphatidylcholines in Mouse Brain by Imaging Mass Spectrometry. *J. Lipid Res.* **50**, 1776–1788 (2009)
- Murphy, R.C., Hankin, J.A., Barkley, R.M.: Imaging of Lipid Species by MALDI Mass Spectrometry. *J. Lipid Res.* **50**, S317–S322 (2009)
- Astigarraga, E., Barreda-Gómez, G., Lombardero, L., Fresnedo, O., Castaño, F., Giral, M.T., Ochoa, B., Rodríguez-Puertas, R., Fernández, J.A. Profiling and Imaging of Lipids on Brain and Liver Tissue by Matrix-Assisted Laser Desorption/ Ionization Mass Spectrometry Using 2-Mercaptobenzothiazole as a Matrix. *Anal. Chem.* **80**, 9105–9114 (2008)
- Deeley, J.M., Hankin, J.A., Friedrich, M.G., Murphy, R.C., Truscott, R.J., Mitchell T, W.; Blanksby, S. J.: Sphingolipid Distribution Changes with Age in the Human Lens. *J. Lipid Res.* **51**, 2753–2760 (2010)
- Grey, A.C., Gelasco, A.K., Section, J., Moreno-Rodríguez, R.A., Krug, E.L., Schey, K.L.: Molecular Morphology of the Chick Heart Visualized by MALDI Imaging Mass Spectrometry. *Anat. Rec. (Hoboken)* **293**, 821–828 (2010)
- Hankin, J.A., Murphy, R.C.: Relationship Between MALDI IMS Intensity and Measured Quantity of Selected Phospholipids in Rat Brain Sections. *Anal. Chem.* **82**, 8476–8484 (2010)
- Burnum, K.E., Cornett, D.S., Puolitaival, S.M., Milne, S.B., Myers, D.S., Tranguch, S., Brown, H.A., Dey, S.K., Caprioli, R.M.: Spatial and Temporal Alterations of Phospholipids Determined by Mass Spectrometry During Mouse Embryo Implantation. *J. Lipid Res.* **50**, 2290–2298 (2009)
- Sparvero, L.J., Amoscato, A.A., Kochanek, P.M., Pitt, B.R., Kagan, V. E., Bayir, H.: Mass-Spectrometry Based Oxidative Lipidomics and Lipid Imaging: Applications in Traumatic Brain Injury. *J. Neurochem.* **115**, 1322–1336 (2010)
- Frey, L.C., Hellier, J., Unkart, C., Lepkin, A., Howard, A., Hasebroock, K., Serkova, N., Liang, L., Patel, M., Soltesz, I., Staley, K.: A Novel

- Apparatus for Lateral Fluid Percussion Injury in the Rat. *J. Neurosci. Methods* **177**, 267–272 (2009)
15. Farias, S., Frey, L.C., Murphy, R.C., Heidenreich, K.A.: Injury-Related Production of Cysteinyl-Leukotrienes Contributes to Brain Damage Following Experimental Traumatic Brain Injury. *J. Neurotrauma* **26**, 1977–1986 (2009)
  16. Perri, B.R., Smith, D.H., Murai, H., Sinson, G., Saatman, K.E., Raghupathi, R., Bartus, R.T., McIntosh, T.K.: Metabolic Quantification of Lesion Volume Following Experimental Traumatic Brain Injury in the Rat. *J. Neurotrauma* **14**, 15–22 (1997)
  17. Spencer, S.J., Auer, R.N., Pittman, Q.J.: Rat Neonatal Immune Challenge Alters Adult Responses to Cerebral Ischaemia. *J. Cereb. Blood Flow Metab.* **26**, 456–467 (2006)
  18. Hankin, J.A., Barkley, R.M., Murphy, R.C.: Sublimation as a Method of Matrix Application for Mass Spectrometric Imaging. *J. Am. Soc. Mass Spectrom.* **18**, 1646–1652 (2007)
  19. Jurche, J.C., Rubakhin, S.S., Sweedler, J.V.: MALDI-MS Imaging of Features Smaller than the Size of the Laser Beam. *J. Am. Soc. Mass Spectrom.* **16**, 1654–1659 (2005)
  20. Kirino, T.: Delayed Neuronal Death in the Gerbil Hippocampus Following Ischemia. *Brain Res.* **239**, 57–69 (1982)
  21. Pulsinelli, W.A., Brierley, J.B., Plum, F.: Temporal Profile of Neuronal Damage in a Model of Transient Forebrain Ischemia. *Ann. Neurol.* **11**, 491–498 (1982)
  22. Petito, C.K., Feldmann, E., Pulsinelli, W.A., Plum, F.: Delayed Hippocampal Damage in Humans Following Cardiorespiratory Arrest. *Neurology* **37**, 1281–1286 (1987)
  23. Zola-Morgan, S., Squire, L.R., Amaral, D.G.: Human Amnesia and the Medial Temporal Region: Enduring Memory Impairment Following a Bilateral Lesion Limited to Field CA1 of the Hippocampus. *J. Neurosci.* **6**, 2950–2967 (1986)
  24. Murphy, R. C., Axelsen, P. H.: Mass Spectrometric Analysis of Long-Chain Lipids. *Mass Spectrom. Rev.* **2010**, in press.
  25. Nakane, M., Kubota, M., Nakagomi, T., Tamura, A., Hisaki, H., Shimasak, H., Ueta, N.: Lethal Forebrain Ischemia Stimulates Sphingomyelin Hydrolysis and Ceramide Generation in the Gerbil Hippocampus. *Neurosci. Lett.* **296**, 89–92 (2000)
  26. Jackson, S.N., Ugarov, M., Post, J.D., Egan, T., Langlais, D., Schultz, J. A., Woods, A.S.: A Study of Phospholipids by Ion Mobility TOFMS. *J. Am. Soc. Mass Spectrom.* **19**, 1655–1662 (2008)
  27. Jackson, S.N., Wang, H.Y., Woods, A.S.: In Situ Structural Characterization of Glycerophospholipids and Sulfatides in Brain tissue using MALDI-MS/MS. *J. Am. Soc. Mass Spectrom.* **18**, 17–26 (2007)
  28. Chen, Y., Allegood, J., Liu, Y., Wang, E., Cachón-Gonzalez, B., Cox, T.M., Merrill Jr., A.H., Sullards, M.C.: Imaging MALDI Mass Spectrometry Using an Oscillating Capillary Nebulizer Matrix Coating System and Its Application to Analysis of Lipids in Brain from a Mouse Model of Tay-Sachs/Sandhoff Disease. *Anal. Chem.* **80**, 2780–2788 (2008)
  29. Vestal, M.L.: Modern MALDI Time-of-Flight Mass Spectrometry. *J. Mass Spectrom.* **44**, 303–317 (2009)
  30. Kubota, M., Narita, K., Nakagomi, T., Tamura, A., Shimasaki, H., Ueta, N., Yoshida, S.: Sphingomyelin Changes in Rat Cerebral Cortex During Focal Ischemia. *Neurol. Res.* **18**, 337–341 (1996)
  31. Taya, K., Marmarou, C.R., Okuno, K., Prieto, R., Marmarou, A.: Effect of Secondary Insults Upon Aquaporin-4 Water Channels Following Experimental Cortical Contusion in Rats. *J. Neurotrauma* **27**, 229–239 (2010)
  32. Durmaz, R., Kanbak, G., Akyüz, F., Isiksoy, S., Yücel, F., Inal, M., Tel, E.: Lazaroid Attenuates Edema by Stabilizing ATPase in the Traumatized Rat Brain. *Can. J. Neuro. Sci.* **30**, 143–149 (2003)